

Experimental investigation on ultra-low power metamaterial for back-scatter communication through ice

Haobin Yang,¹ Tongyu Ding,¹ Shaoqing Zhang,² Longfang ye,³ and Liang Zhang¹

¹School of Ocean Information Engineering, Jimei University, Xiamen 361021, China

²Shenyang Aircraft Design and Research Institute, Shenyang 110035, China

³Institute of Electromagnetics and Acoustics Xiamen University, Xiamen 361005, Fujian, China
Email: liangzhang@jmu.edu.cn

Wireless sensor networks and nodes are faced with severe constraints in power capacity and lifespan, especially in harsh and cold environments. Electromagnetic radiation energy harvesters serve as a promising alternative power source for sensor nodes. However, the power output from reported energy harvesters remains limited, emphasizing the critical need to reduce power consumption in sensor nodes. In this study, we propose a miniaturized low-voltage controllable metamaterial. It is intended for 2.4 GHz wireless band and is capable of operating in extremely adverse conditions, for instance, beneath the ice, while requiring only 3.3 V control voltage and consumes about 0.3 μ W energy. Measurements in sub-ice environment demonstrate its outstanding reflection control characteristics, making it highly suitable as a backscatter communication node in wireless sensor networks in harsh environments.

Introduction: The environment beneath ice layers holds significant scientific value [1, 2]. Wireless sensors offer prospects for sustained and distributed sensing in sub-ice environments, where wireless nodes collect data and transmit it to base stations using radio frequency (RF) electromagnetic communication [3–5]. The large amount of wireless nodes are intended to operate from months to several years. They have small sizes and are usually difficult for maintenance and replacement. Increasing battery size to guarantee enough energy throughout the node's life-cycle would enlarge both the volume and costs.

Recent research has proposed integrating energy harvesters with wireless sensor networks to enhance sufficient energy and thereby extending power lifetimes [6, 7]. Energy harvesters gather energy from the environment, utilizing sources such as vibration energy, thermal energy, light, or RF radiation [8, 9]. In cold environments far from urban areas, RF radiation energy harvesting has emerged as a primary choice for powering sub-ice sensor nodes, demonstrating their capabilities in energy acquisition ranging effectively from 200 μ W to 1 mW [10–12]. However, energy harvesters provide limited power, posing ongoing challenges for power supply. To achieve energy autonomy throughout the network's lifecycle, minimizing network power consumption is badly needed.

Backscatter communication systems or elements, particularly those based on varactor diodes, eg. active frequency selective surfaces (AFSS), exhibit extremely low power consumption due to their passive nature, achieving power levels in the range of microWatt and milliWatt [13]. The high bias voltage required by AFSS varactors makes it unable to be powered solely by energy harvesters [14]. As is reported by state-of-the-art literature, existing AFSSs normally operate at a control voltage level of up to 30 V [15–17], which exceeds the capacity of energy harvester and is not compatible with wireless network nodes supply voltage standard. Specialized boost circuits are required, but lead to issues of circuit complexity, high cost, and energy loss. To address these concerns, we propose developing AFSS units that operate at a low bias voltage, ranging from 0 to 3.3 V, and evaluating their performance in extremely cold environments.

In this paper, we proposed a miniaturized, low-power AFSS under standard node voltage control. This enables the AFSS to use energy from energy harvesters directly, achieving self-sufficiency for wireless sensor nodes and reducing dependence on external power sources and maintenance costs. The fabricated prototype is then tested in ice environment,

demonstrating its capability as ultra-low-power node modules in sub-ice wireless network applications.

Antenna Design: The AFSS adopts the classical ELC structure for the unit and it introduces a zigzag structure to enhance coupling between units, achieving miniaturization goals. Utilizing Infineon's BB857 varactor diode as a pivotal component, the design is validated through full-wave simulations. As shown in Figure 1(a), the red circle represents a 10k resistor, and the black rectangle represents an Infineon BB857 varactor with a reverse bias voltage capacitance of 3.4 pF at 3.3 V and a reverse resistance of 4342 M Ω . At high frequencies, the resulting surface current forms a zigzag pattern, bypassing the resistor and flowing through the varactors. The detailed dimensions are given in Figure 1(b). It adopts a single-layer structure, with the substrate material being FR-4, and the size of unit cell are only 5.5 \times 5.6 mm². The proposed saw-tooth structure effectively enhances the magnetic field coupling between AFSS units, thereby achieving effective miniaturization of the AFSS unit. In this study, a series connection method was used to create the prototype, with each column consisting of six units, making the total length of 37 mm. This study controls the high-frequency path by increasing the resistance, and the excellent design of the series connection eliminates the need for a bias network, thereby avoiding the impact of the bias grid on the frequency response.

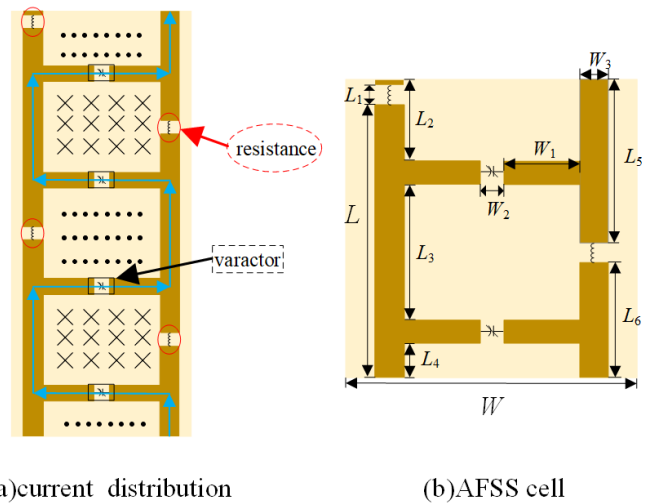


Fig 1 Current distribution of zigzag structure under HF path. Fig. 1 (a) Current distribution of the zigzag structure under HF path. (b) The dimension of the AFSS unit cell ($L = 5.2$ mm, $L_1 = 0.4$ mm, $L_2 = 1$ mm, $L_3 = 2.4$ mm, $L_4 = 1$ mm, $L_5 = 2.8$ mm, $L_6 = 2.4$ mm, $W = 5.5$ mm, $W_1 = 1.5$ mm, $W_2 = 0.4$ mm, $W_3 = 0.4$ mm).

Simulation results: Given the relative permittivity of ice is $\epsilon_r = 3.2$ and the dissipation factor is $\tan \delta = 0.0009$. We have simulated the performance of AFSS placed in ice via CST frequency domain solver to evaluate its suitability for sub-ice environments. The simulation results show that the AFSS in ice maintains a stable reflection coefficient in the range of 2.26–2.5 GHz, with reflection loss remaining around -1 dB. Due to the low permittivity of ice, the wavelength of electromagnetic wave is relatively increased, causing the center frequency of the reflection coefficient to shift to higher frequencies slightly. As shown in Figure 2, through simulation verification, we inferred that AFSS is suitable and reliable in sub-ice environments. Considering a bias voltage of 3.3 V and a reverse resistance of 4342 M Ω , the total power consumption of the AFSS, composed of ten AFSS columns in this study, is approximately 0.3 μ W. The proposed AFSS screens have a total power consumption of 0.3 μ W and control voltages that accord with standard node voltages.

The radiation pattern, shown in Figure 3, vividly illustrates that as the operational frequency increases, the main lobe of the antenna progressively shifts towards higher angles, ultimately achieving a scanning range of 0° to 10° within a 4 GHz bandwidth.

Prototyping and experimental verification: As shown in Figure 3(b), we fabricated an AFSS array, with each column measuring $5.5 \times 37 \text{ mm}^2$, approximately one-third of the wavelength. The prototype underwent experimental validation while embedded in ice to assess its reflection change rate, which serves as a pivotal performance metric for the backscatter communication systems.

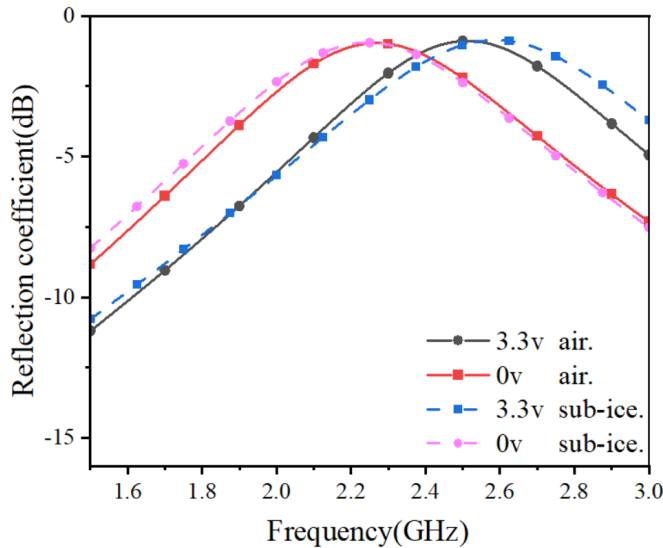
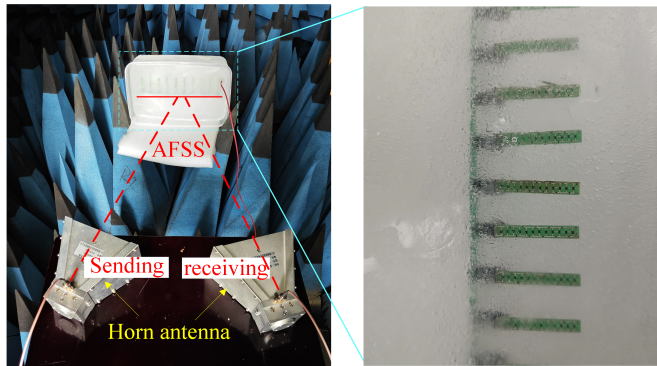


Fig 2 The full wave simulation of reflection coefficient of AFSS (air and in-ice condition).



(a) Measurement environment (b) Fabricated prototype

Fig 3 The AFSS and measurement environment fabricated prototype.

Figure 3 depicts the measurement environment. The AFSS screen is embedded in the ice. Two horn antennas are positioned at the same height as the AFSS screen and oriented towards it. These antennas are connected to the Vector Network Analyzer (VNA), with one antenna connected to port 1 and the other to port 2. Then we used the so-called thru mode calibration method to test the reflection rate of the screen. As is known, the thru mode calibration method is capable of eliminating the errors caused by circuits near the ports. It conducts two single tests and gives the reflection rate results by subtracting the two groups of data. In this sense, we set the measurement environment according to Figure 3(a) and applied 0 V bias voltage to the AFSS screen first, then we adjusted the VNA to tune the measured S21 to a horizontal line, which is used as a baseline later. Next, we applied a 3.3 V bias voltage to the AFSS screen and the measured S21 is straightforward the difference of results under the two bias voltages, namely, the variation of reflection rate, as is shown in Figure 4. Since we focused on the modulation capability of the screen at 2.4 GHz, it is evident from Figure 4 that at the 2.4 GHz single frequency point, the power signal increases by more than 3 dB. Both simulated and measured results show that the AFSS proposed in this study exhibits excellent reflection control characteristics, making it highly suitable for wireless sensor network nodes within energy

harvesting systems. This design not only offers advantages in size and power consumption but also significantly improves manufacturing cost-effectiveness and practical utility.

Both simulated and measured results show that the AFSS proposed in this study exhibits excellent reflection control characteristics, making it highly suitable for wireless sensor network nodes within energy harvesting systems. This design not only offers advantages in size and power consumption but also significantly improves manufacturing cost-effectiveness and practical utility.

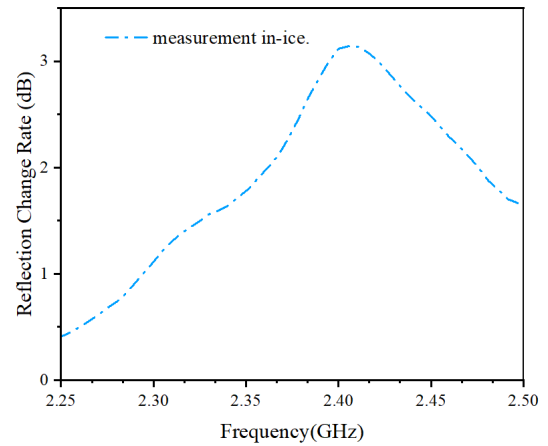


Fig 4 Measurement of 0 to 3.3 V reflection change rate in-ice environment.

Conclusion: This study proposes a low-power, low-voltage controlled AFSS suitable for backscatter communication systems as wireless sensor nodes. The research simulates and elucidates surface currents in resonance states, with simulation results indicating that the center frequency of the stop band can be tuned within the range of 2.26 to 2.5 GHz. Subsequently, a prototype of this design was fabricated. Measurements conducted with the prototype immersed in ice block showed that the reflectivity exceeds 3 dB at the 2.4 GHz frequency point when bias voltages range from 0 to 3.3 V. Backscatter communication systems exhibit extremely low power consumption due to their passive radiation nature, particularly with the proposed AFSS in this study consuming only 0.3 μW , significantly less than the power provided by RF energy harvesters. This offers a potential solution to power issues for wireless sensor nodes under ice layers.

Acknowledgments: This work is supported by the Natural Science Foundation of Xiamen under grant number 3502Z20227209 and the Natural Science Foundation of Fujian Province under grant number 2023J01808, and Fujian Provincial Key Laboratory of Oceanic Information Perception and Intelligent Processing.

© 2024 The Authors. *Electronics Letters* published by John Wiley & Sons Ltd on behalf of The Institution of Engineering and Technology

This is an open access article under the terms of the Creative Commons Attribution License, which permits use, distribution and reproduction in any medium, provided the original work is properly cited.

Received: 10 January 2021 Accepted: 4 March 2021

doi: 10.1049/ell2.10001

References

1. Wiltshire, B., et al., Robust and sensitive frost and ice detection via planar microwave resonator sensor. *Sensors and Actuators B: Chemical* 301, 126881 (2019)
2. Tariq, R. U., et al., Microwave Sensor for Detection of Ice Accretion on Base Station Antenna Radome. *IEEE Sensors Journal* 21(17), 18733–18741 (2021)
3. Kozak, R., et al., Patch Antenna Sensor for Wireless Ice and Frost Detection. *Sci. Rep.* 11(13707) (2021).
4. Wagih, M., et al., Wireless ice detection and monitoring using flexible UHF RFID tags. *IEEE Sensors J* 21(17), 18715–18724 (2021)

5. Shi, J., et al., Flexible direct-write printed RF sensor for RF ice sensing, *Proc. IEEE Int. Conf. Flexible Printable Sens. Syst. (FLEPS)*, 1–4 (2021)
6. Ruan, T., et al., Energy-Aware Approaches for Energy Harvesting Powered Wireless Sensor Nodes. *IEEE Sensors Journal* 17(7), 2165–2173 (2017)
7. Sah, D. K., et al., An Efficient Routing Awareness Based Scheduling Approach in Energy Harvesting Wireless Sensor Networks. *IEEE Sensors Journal* 23(15), 17638–17647 (2023)
8. Vullers, R.J.M., et al., Micropower energy harvesting. *Solid-State Electronics* 53(7), 684–693 (2009).
9. Vullers, R.J.M., et al., RF harvesting using antenna structures on foil, *Proceedings of Power MEMS 2008*, 209–212 (2008)
10. Ungan, T., et al., Harvesting low ambient rf-sources for autonomous measurement systems. In: *Proceedings of I2MTC 2008 IEEE International Instrumentation and Measurement Technology Conference*, May 1215, 2008.
11. Arrawatia, M., et al., Differential Microstrip Antenna for RF Energy Harvesting. *IEEE Transactions on Antennas and Propagation* 63(4), 1581–1588 (2015)
12. Shieh, S., et al., Fast Start-Up RF Energy Harvester Design for GSM-900 Uplink Band. *IEEE Transactions on Circuits and Systems II: Express Briefs* 66(4), 582–586 (2019)
13. Zhang, L., et al., Broadband Tunable Frequency Selective Surface for Steerable Antenna Applications. *IEEE Transactions on Antennas and Propagation* 64(12), 5496–5500 (2016)
14. Arrawatia, M., et al., Broadband Bent Triangular Omnidirectional Antenna for RF Energy Harvesting. *IEEE Antennas and Wireless Propagation Letters* 15, 36–39 (2016)
15. Ding, T., et al., Adaptive High-Level Isolation Between Two Closely Placed Copolarized Antennas Using Tunable Screen. *IEEE Antennas and Wireless Propagation Letters* 16, 1016–1019 (2017)
16. Phon, R., et al., Active Frequency Selective Surface to Switch Between Absorption and Transmission Band With Additional Frequency Tuning Capability. *IEEE Transactions on Antennas and Propagation* 67(9), 6059–6067 (2019)
17. Guo, Q., et al., Active Frequency Selective Surface With Wide Reconfigurable Passband. *IEEE Access* 7, 38348–38355 (2019)